INTERACTION BETWEEN NONLINEAR WATER WAVES AND STRUCTURES WITH FLARE

C.Z. Wang and G.X. Wu*
Department of Mechanical Engineering, UCL, Torrington Place, London WC1E 7JE, UK
*Tel. 00-44-(0)20-76793870, Fax 00-44-(0)20-73880180 email: gx_wu@meng.ucl.ac.uk

INTRODUCTION

There have been extensive applications of FEM to nonlinear wave and floating body interactions recently. A typical example in this area is the simulation of interaction between waves and fixed structures in numerical tanks (Ma, Wu and Eatock Taylor 2001a, b). Hu, Wu and Ma (2002) extended this method to the case that a cylinder is in forced motion. Both of these two works are based on structured meshes with connectivities between nodes remaining unchanged during the simulation. More recently, Wu and Hu (2003) considered a floating structure in large amplitude motion. A hybrid mesh, with the unstructured near the body and the unstructured away from the body, is used. A completely new grid is generated regularly and information is transported from one mesh to another. All these works, however, are for cylindrical structures with no variation of the cross section in the vertical direction.

For the problem of steep wave interaction with structures, important topics of interest are wave impact at the bows of FPSOs and green water loading. A noticeable feature in FPSO design is the large bow with pronounced flare above the still waterline. A greater flare can improve the performance of ships by increasing local reserve of buoyancy and limiting the green water on deck (Schneekluth and Bertram, 1998). With such a change in design, traditional prediction methods become less reliable and direct numerical simulation would be more appropriate. However, flare could cause a rapid variation in pressure especially when the relative angle between the structure and the free surface is small. Some certifying authorities call for additional localized strengthening to be incorporated in FPSO vessels with a rounded bow and flare. The hydrodynamic forces on the flared structure may have stronger nonlinearity than those without flare. This will make the simulation more difficult and complex. The aim of the present study is to develop a finite element based numerical method to investigate the interaction between waves and flared structures using the fully nonlinear wave theory. The study is also relevant to the assessment of ringing vibration of monotower structures that incorporate flare above the still water level (e.g. Draugen platform).

MATHEMATICAL FORMULATION

A numerical wave tank with length L, width B and depth h is shown in Fig. 1. The x-axis of the coordinate system is along the longitudinal direction of the tank, z-axis is positive upwards and the origin is on the undisturbed free surface. The fluid is assumed to be inviscid and incompressible, and the flow is irrotational. Velocity potential ϕ in the fluid domain therefore satisfies the Laplace equation,

$$\nabla^2\phi = 0. \tag{1}$$

On the instantaneous free surface, the dynamic and kinematic conditions can be described by the Langrangian form

$$\frac{D\phi}{Dt} = -g\eta + \frac{1}{2}\nabla\phi\nabla\phi, \tag{2}$$

$$\frac{Dx}{Dt} = \frac{\partial\phi}{\partial x}, \frac{Dy}{Dt} = \frac{\partial\phi}{\partial y}, \frac{Dz}{Dt} = \frac{\partial\phi}{\partial z}, \tag{3}$$

where g is the acceleration due to the gravity and η is the wave elevation.

On the wave maker, the condition is prescribled as

$$\frac{\partial\phi}{\partial n} = \boldsymbol{U_0}\cdot\boldsymbol{n}, \tag{4}$$

where $\boldsymbol{U_0}$ is the the velocity of the wave maker and $\boldsymbol{n}$ is its normal vector pointing out of the fluid domain. The boundary condition on the moving body surface is

$$\frac{\partial\phi}{\partial n} = \boldsymbol{V}\cdot\boldsymbol{n}. \tag{5}$$

On the side wall and bottom of the tank, the boundary condition is

$$\frac{\partial\phi}{\partial n} = 0. \tag{6}$$

The radiation condition at the far end is imposed through a damping zone and sommerfeld condition. The initial

conditions should be given since the problem is solved in time domain

$$\phi(x, y, z = \xi, t = 0) = \phi_0(x), \quad \eta(x, y, t = 0) = \xi(x, y) . \quad (7)$$

FINITE ELEMENT DISCRETIZATION AND NUMERICAL PROCEDURES

An essential part of CFD is the mesh generation. As mentioned in Wu & Hu (2003), a fully 3D grid generator is usually too computationally intensive for this problem, as a typical simulation would allow a few minute CPU at each time step. Thus, they adopted a 2D method for cylindrical structures. The mesh is first obtained through the tri-tree method on a horizontal plane and the 3D mesh is then generated by drawing straight lines in the vertical direction. The procedure is efficient but it does not allow variation of cross section in the vertical direction, even though the shape of the section can be arbitrary.

When the body has a flare, substantial change in mesh generation is required. For a cylindrical structure, the projection of the waterline on the free surface will remain the same if the body is in translation only. For a flared structure, the projection will vary considerably. We summarize the mesh generation project below.

1. The wavy free surface is first projected to the horizontal plane. A 2D mesh generator called BAMG (Hecht, 1998) is then used, which is based on the Delaunay algorithm. One of its advantages is that it is less computational intensive.

2. The horizontal coordinates are used to locate nodes on the free surface, using interpolation if necessary.

3. A curve is then drawn along the depth to form the 3D mesh. We use prisms instead of tetrahedral elements here. One of the advantages of this element is that its index system is much simpler for this problem.

The procedure of the mesh generation is shown in figure 2 to 6. It should be noted that there is a zone of structured mesh near the wave maker. The reason of its presence is due to the transverse stability discussed by Wu, Ma & Eatock Taylor (1996). They found that the stability depends very much on the mesh structure used near the wave maker and the one shown in figure 4 is most stable among many choices.

After the mesh is generated, we can solve the problem using the finite element method. The coordinate $\boldsymbol{x} = (x, y, z)$ in the fluid domain and the velocity at $\boldsymbol{x}$ can be expressed using shape function N_i

$$\boldsymbol{x} = \sum_{i=1}^{6} N_i \boldsymbol{x}_i , \quad (8)$$

$$\phi = \sum_{i=1}^{6} N_i \phi_i(\boldsymbol{x}) . \quad (9)$$

The finite element equation can be derived by using the Galerkin method

$$[K]\{\phi\}=\{F\}, \quad (10)$$

where

$$k_{ij} = \iiint_{\forall} \nabla N_i \cdot \nabla N_j d\forall ,$$

$$\{\phi\} = [\phi_1, \phi_2, \ldots, \phi_n] ,$$

$$f_j = \iint_s \frac{\partial \phi}{\partial n} N_j ds .$$

Here we use the 6-node shape function with the prism element discussed previously. As a result, the global matrix is calculated through numerical integration. This is different from the 4-node linear shape function with the tetrahedral element where the integration can be done analytically. The feature here is that the procedure can be used by higher order elements. Once the coefficients in the matrix have been found, Eq. (10) is solved by the PCG iterative method with SSOR preconditioner.

When tracking the wavy motion and calculating force, the velocity on the free surface and body surface are needed at each time step. Ma, Wu and Eatock Taylor(2001a, b) presented a method which requires the node on the free surface and two nodes immediately below the free surface on the same vertical line. The method is found to be accurate but it is suitable only for a cylindrical structure. For the flared structure, the method developed by Wu and Eatock Taylor (1994) when they considered the 2D problem is adopted. We first expand the velocity in terms of the shape function similar to Eq. (9). Galerkin method is then used

$$\iiint_{\forall} (\mathbf{u} - \nabla \phi) N_i d\forall = 0 \quad (11)$$

This gives

$$[A]\{\mathbf{u}\} = [B]\{\phi\}, \quad (12)$$

where

$$a_{ij} = \iiint_{\forall} N_i N_j d\forall ,$$

$$b_{ij} = \iiint_{\forall} N_i \nabla N_j d\forall .$$

This method removes the restriction mentioened above but the penalty is that one has to solve another linear equation.

Finally the first order Adams-bashforth scheme is adopted to update the velocity potential and the locations of the free surface

$$f(t + \Delta t) = f(t) + \frac{\Delta t}{2}[\, 3f'(t) - f'(t - \Delta t)] . \quad (13)$$

The method developed by Wu and Eatock Taylor (1996, 2003) is employed to calculate the force and the body motion.

NUMERICAL EXAMPLES

In all the simulations, the depth h of the tank is used to dimensionalize the length. The tank length L is 12, and breadth B is 0.72. The radius r of all cylinders is 0.1416. The body is located at a distance of L_{wc}=7 away from the wave maker, and the length of damping zone is selected as $L_{dm}=2\lambda$ (λ is wavelength). When the body has flare, the variation of the cross section starts from z=-0.25. The dimension of the truncated cylinder is shown in Fig. 7. The wave maker is assumed to be subject to the following horizontal harmonic motion

$$x = -a\cos(\omega t), \qquad (14)$$

where a is the amplitude of motion, and ω is the frequency.

In all computations, the nodimensional frequency $\omega/\sqrt{g/h}$ is set to be 2.0. A typical wave profile around the flared cylinder is shown in Fig. 8. Fig. 9 shows the history of wave at the front of a bottom mounted flared cylinder with three different amplitudes a=0.01, 0.02 and 0.03. In the figure, τ is nodimensional time and defined as $\tau = t/\sqrt{h/g}$. The nonlinear effect is evident. Fig. 10 shows the comparison of wave histories between the truncated and the bottom mounted cylinders with flare. There is no obvious difference between the two cases, which is expected as deeply submerged part of the body has little effect on waves. A comparison of hydrodynamic force between bottom mounted cylinders with and without flare is shown in Fig. 11. The force f and moment m about the bottom of the cylinder in the figure are defined as $f = \text{force}/\rho g r^2 a$ and $m = \text{moment}/\rho g r^2 a h$.

A major difference in results for cylinders with and without flare is the vertical force which obviously does not exist or is very small for the former. Fig. 12 gives the vertical force (excluding the static force) when a=0.02. It shows that the vertical force contains higher harmonic components. The history of the force for both bottom mounted and truncated cylinders is shown in Fig. 13.

ACKNOWDEDGEMENT

This work is supported by EPSRC (GR/R26719/01) through a joint project with Professor Robin Langley of University Of Cambridge, to which the authors are most grateful. The authors are also grateful to Dr Kevin Drake for his valuable input on the design and hydrodynamic issues of a flared structure.

REFERENCES

1. Hecht F (1998), BAMG: Bidimensional anisotropic mesh generator, website: http://www-rocq1.inria.fr/gamma/cdrom/www /bamg/eng.htm
2. Hu P.X., Wu G.X. and Ma QW (2002), "Numerical simulation of nonlinear wave radiation by a moving vertical cylinder", *Ocean Eng*. Vol.29, pp.1733-1750
3. Ma Q.W., Wu G.X. and Eatock Taylor R. (2001a), "Finite element simulation of fully nonlinear interaction between vertical cylinders and steep waves. Part 1: Methodology and numerical procedure", *Int. J. for Num. Methods in Fluids*, Vol. 36, pp. 265-285.
4. Ma Q.W., Wu G.X. and Eatock Taylor R. (2001b), "Finite element simulation of fully nonlinear interaction between vertical cylinders and steep waves. Part 2: Numerical results and validation", *Int. J. for Num. Methods in Fluids*, Vol. 36, pp. 287-308.
5. Schneekluth H. and Bertram V. (1998), *Ship Design for Efficiency & Economy*, 2th edition, Butterworth-Heinemann, Oxford.
6. Wu G.X. and Eatock Taylor R. (1994), "Finite element analysis of two-dimensional non-linear transient water waves", *Applied Ocean Research*, Vol. 16, pp. 363-372.
7. Wu, G.X. and Eatock Taylor, R. (1996), "Transient motion of a floating body in steep water waves", *Proc.11th Workshop on water waves and Floating Bodies*, Hamburg.
8. Wu, G.X. and Eatock Taylor, R. (2003) "The coupled finite element and boundary element analysis of nonlinear interactions between waves and bodies" *Ocean Eng.* , Vol.30, pp. 387-400
9. Wu G.X. and Hu Z.Z. (2003), Simulation of Nonlinear Interactions between Waves and Floating Bodies through a Finite Element Based Numerical Tank. *Submitted for publication*.
10. Wu, G.X., Ma, Q.W. and Eatock Taylor, R (1996) "analysis of interactions between nonlinear waves and bodies by domain decomposition" *21st Symp. on Naval Hydrodynamics*, Trondheim, Norway

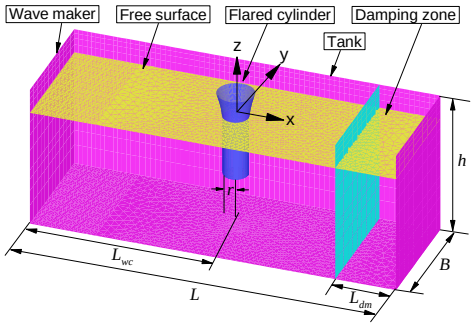

Fig. 1 Computational domain for a numerical tank

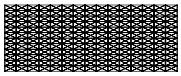

Fig. 2 2D structured mesh

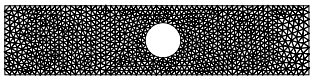

Fig. 3 2D unstructured mesh

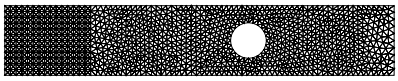

Fig. 4 2D hybrid mesh

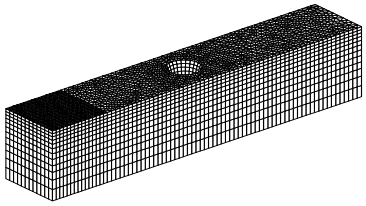

Fig. 5 3D mesh for one cylinder

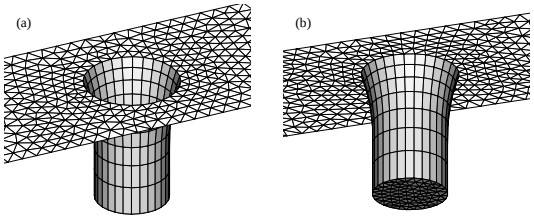

Fig 6 Surface mesh on a truncated cylinder with flare

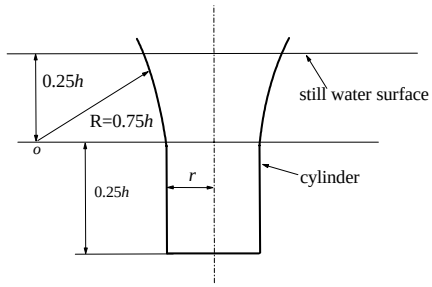

Fig. 7 Dimension of the truncated cylinder with flare

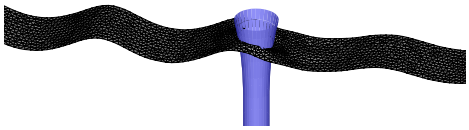

Fig. 8 Wave profile around the flared cylinder

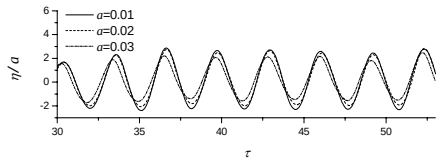

Fig. 9 Time history of wave at the front side of the bottom mountedcylinder with flare

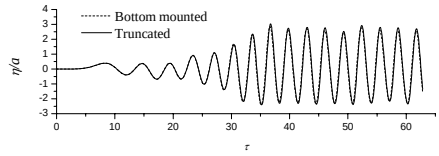

Fig. 10 Time history of wave at the front side of the cylinder with flare at a=0.01

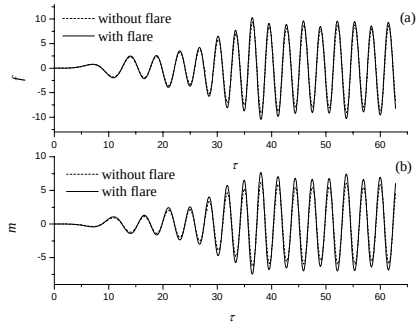

Fig.11 Hydrodynamic force on the bottom mounted cylinder at a=0.01
(a) force in x-direction; (b) moment

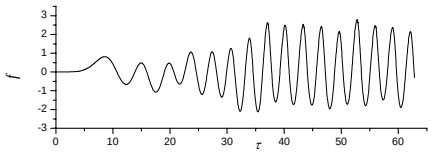

Fig. 12 Vertical force on the bottom mounted cylinder at a=0.02

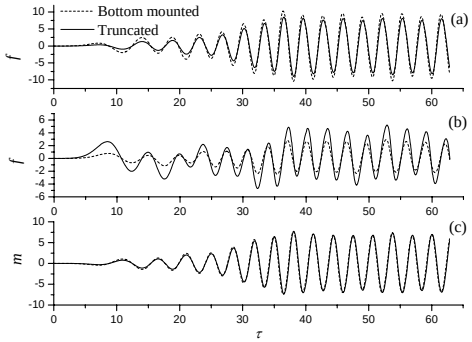

Fig. 13 Time history of force on the cylinder with flare at a=0.01
(a) force in x-direction; (b) force in y-direction; (c) moment